Analytical Modeling of Low-Loss Disk Flexure Resonators

Jonathan M. Puder
OxideMEMS Lab
Cornell University
Ithaca, USA

Jeffrey S. Pulskamp, Ryan Q. Rudy, and Ronald G. Polcawich
Sensors and Electron Devices Directorate
US Army Research Laboratory
Adelphi, USA

Sunil A. Bhave
OxideMEMS Lab
Purdue University
West Lafayette, IN

***Abstract*—This paper presents for the first time a closed form analytical solution for the motional resistance, R_m, of the transverse (1,1) mode of two port disk flexure resonators (DFRs), enabling rapid performance prediction and device optimization. This work is motivated by a recently reported -1 dB peak S_{21} and 9 Ω motional resistance DFR that has demonstrated the viability of non-traditional flexure based modes as high-performance, low frequency MEMS resonators. Modeled R_m values are validated using on-wafer extracted e_{31} piezoelectric stress constants, measured layer thicknesses, independently measured elastic moduli, and analytical mode shapes**

Keywords*— *Motional resistance, piezoelectricity, resonator

I. Introduction

Military communications systems, such as SINCGARS, continue to rely on sub-100 MHz filters, and require IF filters with narrow bandwidth, exceptional stop-band rejection, and frequency trimming capabilities. While early literature focused on flexure-based devices to meet these needs, in recent years research efforts have moved towards other modes. However, recently published resonator performance of -1 dB peak S_{21} and 9 Ω motional resistance (R_m) for six parallel (1,1) PZT-on-silicon [1,2,3,4] disk flexure resonators terminated directly to 50 Ω highlights the potential of flexure-based devices as high-performance resonators at low frequencies [5]. To provide insight into the performance of these modes, this work will present an analytical expression for R_m, an important modeling parameter. This analytical expression is validated by fitting only the mechanical quality factor (Q_m), and using independently measured or extracted parameters, including e_{31}.

II. Theory

A. Motional Resistance

Modal analysis was used to model the (1,1) mode (Fig. 1) of the continuous disk as a driven, lumped mass-spring system by comparing the elastic energies of the two systems as well as the work done by the modal force and piezoelectric stress. Analytical mode shapes of the (1,1) mode of disk flexure consisting of modified and ordinary Bessel functions of the first kind [6], were used to obtain modal stresses and strains. The modal force and equivalent stiffness were used to derive a quasi-static displacement. Then, using extracted mechanical quality factor (Q_m), the frequency response of the predicted real displacement was calculated. Displacement was converted to a frequency- and time-dependent charge on the output port via the direct piezoelectric effect. The application of a time derivative and rearrangement returns the closed-form expression for R_m in Equation (1),

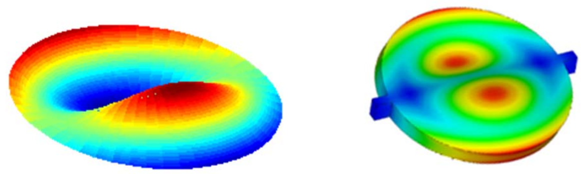

(a) (b)

Fig. 1. The mode shape of disk flexure resonator from (a) FEA Eigen frequency analysis (b) analytical mode shapes expressions.

$$R_m = \frac{4\pi\gamma\lambda^2 t_{tot}^2\sqrt{Y_c\rho_c}}{Q_m\sqrt{3(1-\nu^2)}\left(k\, e_{31} h \int_{A_{el}} \beta\, r\, dr d\theta\right)^2} \qquad (1)$$

β in (1) is given by,

$$\beta = \cos(\theta)\left(J_1(kr) - I_1(kr)\right) \qquad (2)$$

where γ is the ratio of modal mass to total mass, λ is a frequency constant, k is the wavenumber, t_{tot} is the total disk thickness, Y_c and ρ_c are the composite elastic moduli and density, υ is Poisson's ratio, h is the distance from the neutral axis to the mid-plane of the piezoelectric layer, and J_1 and I_1 are the ordinary and modified Bessel functions of the first kind [6]. The model predicts high coupling due to energy transduction through both the e_{31} and e_{32} (e_{31}=e_{32} for PZT and AlN) constants, and motional resistance to be independent of radius.

B. Comparison to Other Low Frequency Modes

To understand the advantages of disk resonators, they are compared and contrasted with two other common modes found at low frequencies. Beam resonators are often designed to excite length extension (LE) modes, and have spurious modes of beam

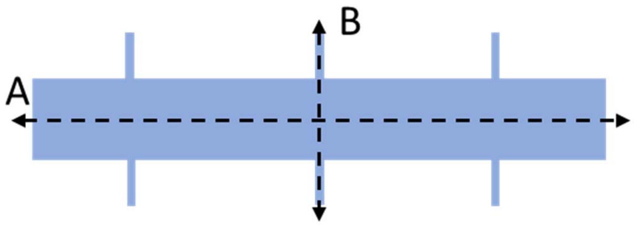

Fig. 2. A top view of the resonator with planes of symmetry marked. Recetangular electrodes are either symmetric about A or symmetric/antisymmetric about B.

flexure (BF). Equations for the motional resistance of these modes are given by [7]

$$R_{m_{Beam\ Flexure}} = \frac{\sqrt{Y_c I \rho_c w_{tot} t_{tot}}}{4LQ_m \left[e_{31} h \int_L \frac{d^2 u_n}{dx^2} w_{el}(x) dx \right]^2} \quad (3)$$

$$R_{m_{Beam\ Extension}} = \frac{n\pi w_{tot} t_{tot} \sqrt{Y_C \rho_c}}{2Q_m \left[e_{31} \int_L \frac{du_n}{dx} w_{el}(x) dx \right]^2} \quad (4)$$

Where the w_{tot} is the total width of the resonator, I is the area moment of inertia, u_n is the unity normalized mode shape of the n^{th} mode, L is the length of the resonator, and w_{el} is the width of the rectangular electrodes. For these expressions, the electrodes are assumed to symmetric or anti symmetric about the planes shown in the schematic of Fig. 2.

Comparing first to beam flexure, both modes are inversely proportional to h^2 and $e_{31}{}^2$. However, the R_m of BF modes scale linearly with L and inversely with w_{tot}, while the disk is not expected to scale with R. However, if L and w_{tot} are changed at the same rate, then the BF R_m is not affected. This approximate relationship would occur as a device is scaled to higher frequencies. Therefore, both modes will have consistent R_m across R and L/w_{tot} ratios. Since R and L are the primary frequency determining dimension in both modes, consistent R_m across a wide range of frequencies should be expected, if t_{tot} is held constant and the L/w_{tot} ratio is maintained. This principle is confirmed in [8], where parameterized simulations of disk resonators with varied widths and silicon thicknesses are run. For both modes, a thicker device with the piezoelectric material far from the neutral axis will result in lower R_m due the scaling with h, assuming that Q_m is not affected by layer thicknesses. However, very thick devices will violate the assumptions used to derive the analytical mode shapes and invalidate the derived R_m expressions. Finally, for both modes, it is possible to have infinite R_m if the neutral axis and midplane of the piezoelectric layer are coincident, since h would be zero. The R_m of BF and DFRs show very similar behavior, which is expected due to both modes being characterized by out of plane flexure.

Comparing DFR R_m and LE R_m, first it is apparent that the LE mode cannot scale with h since this parameter is only defined for flexure resonators. Additionally, the R_m for LE modes can never be infinite in a non-trivial case. The LE mode R_m is expected to scale directly with t_{tot}, while that of the DFR will not have such a clear relation, since h and t_{tot} share a complex relationship. The LE mode R_m is not expected to scale with the primary frequency determining dimension, L, nor is the DFR R_m. However, the LE R_m does scale inversely with the other in plane dimension, w_{el}. Therefore, by maintaining a constant width and changing the length, devices with the same R_m may be fabricated across a wide range of frequencies for LE resonators.

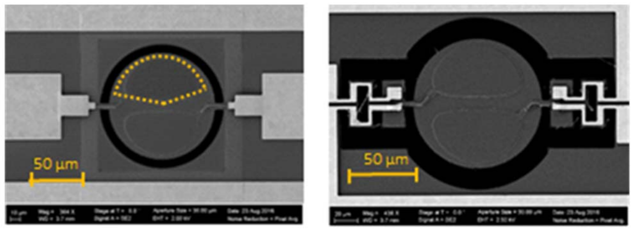

Fig. 3. Micrographs of fabricated devices with both types of anchors. The radius of the disks was 56 µm. The approximated electrode shape used in modeling is traced over Fig. 3a.

III. EXPERIMENTAL VALIDATION

A. Device Details

To validate the derived R_m of the DFRs, devices were fabricated in a PZT on silicon stack [1]. The devices consisted of a 1 µm buried SiO_2 layer, a 10 µm silicon device layer, 300 nm of SiO_2, 125 nm of platinum for the bottom electrode, 0.5 µm of PZT, and 50 nm of platinum for the top electrode. The disks were designed to have a 56 µm radius. Additionally, the disks were fabricated with two types of anchors, which may be seen in Fig 3.

B. e_{31} Piezoelectric Coefficients

Cantilever test structures were used to independently extract the electric-field dependent piezoelectric e_{31} constants under quasi-static conditions [9,10,11]. This field dependence arises directly from the fact that PZT is a ferroelectric material. At 0.5 µm PZT film thickness, the coercive voltage of PZT is less than 2 V. This allows for more rigorous model validation at various operating points due to the fact that the piezoelectric stress constants of PZT can vary between 3-10 C/m^2. The e_{31} were found to vary widely across the wafer, and three examples of extracted coefficients may be seen in Fig. 4.

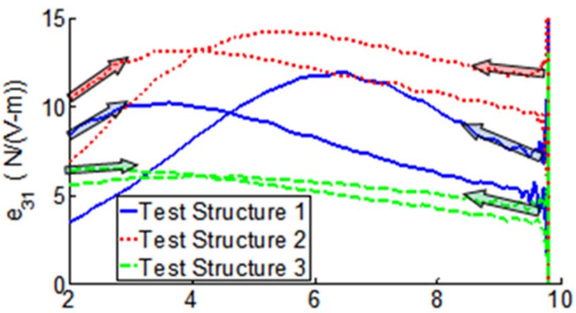

Fig. 4. The e_{31} constants extracted from cantilever test structures. The widely varying cross-wafer values partially explain the variation seen in R_m. The discontinuity at 10V is due to data processing artifacts. Arrows indicate the direction of the unipolar voltage sweep start from 0V up to 10 V and returning to 0V.

The coefficients were extracted using a 90 Hz sine wave with minimum and maximum values of 0 and 10 V, respectively.

Actual devices are operated in a small-AC-on-large-DC signal condition at much higher frequencies. This discrepancy in testing conditions likely contributed to agreement discrepancies in subsequent R_m validation.

C. Measurement and Model Comparison

The scattering parameters of the PZT-on-silicon resonators were measured on a Rhode & Schwarz ZVB8 network analyzer terminated to 50 Ω and calibrated using short, open, load, and through standards (GGB CS-5) with varied superimposed DC biases on both ports. The experimental R_m was extracted by fitting to the well-known modified Butterworth van-Dyke (mBVD) model, and Q_m was extracted via fitting. Tether resistances were obtained via resistivity test structures and combined designed and measured geometries. Using extracted properties, independently measured mechanical material properties [10], and only one fitted parameter (Q_m), values of R_m were calculated (Fig. 5). Frequencies varied from 22.2 to 22.6 MHz at 10V. The extracted R_m varied from 48Ω to 335Ω, which may be attributed to the widely varying e_{31} (Fig. 4) and Q_m. Both e_{31} and Q_m vary cross-wafer and tune with voltage. Although there is a large spread in R_m, the model still matches well without fitting e_{31}. The average error across all voltages was 23%.

D. Predicting High Performance

Fig. 6 plots the predicted S_{21} of device 2 of Fig 5. when placed in parallel six times along with the measured performance of the device from [5] at 8 V. Device 2 was located on the same die as the device from [5]. Since the frequency and shunt capacitance are related to the radius, it is necessary to array the resonators to obtain the desired shunt impedance. This agreement illustrates the ability of this model to accurately predict the behavior of low loss and low R_m devices.

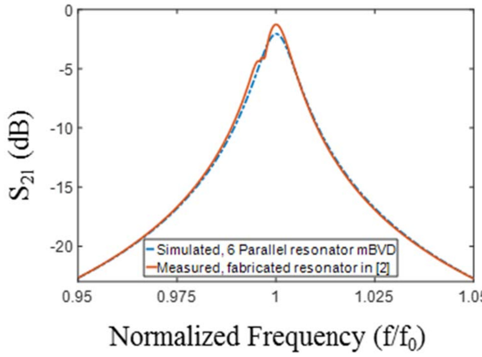

Fig. 6. Simulated S_{21} for Device 2 of Figure 5 in parallel six times, and measured resonator data from the device in [2] at 8V. Both devices were located on the same die. Discrepancies arise from unknown individual disk Q_m, varying e_{31} and center frequency misalignment.

IV. Conclusion

The R_m model presented and validated has provided insight into the design of disk resonators, and has been able to predict the high performance demonstrated in [5]. They are expected to maintain consistent motional resistance across a wide range of frequencies, so long as the device thickness does not approach the radius. Thicker devices with the piezoelectric layer far from the neutral axis are predicted to have a lower R_m as a general trend if Q_m is not affected by relative layer thicknesses. These insights, along with the demonstrated low loss in fabricated devices, warrant a more thorough investigation into the scaling of this family of modes to higher frequencies.

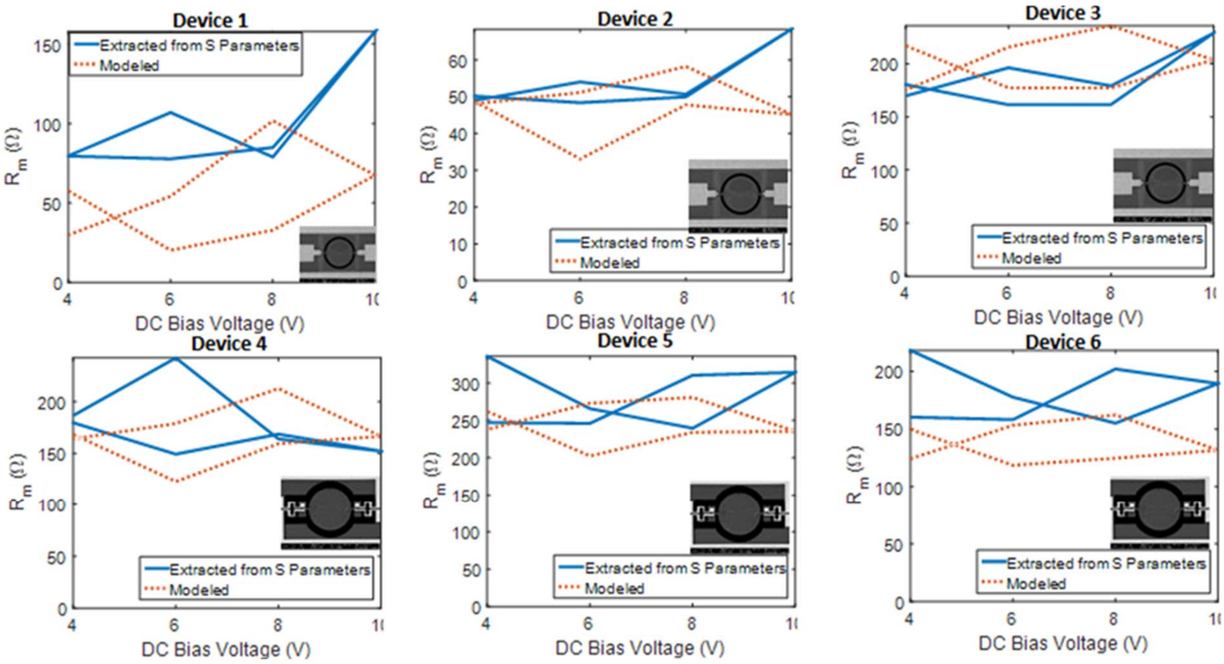

Fig 5. Extracted (solid) and modeled (dashed) R_m. Modeled R_m used extracted e_{31} and Q_m (Fig. 2). Discrepancies in curve shapes is attributed to differences in e_{31} extraction conditions (quasi-static) and RF testing conditions. Overall average error was 23%.

REFERENCES

[1] Pulskamp, J.S., et. al. (2012). "Electrode-shaping for the excitation and detection of permitted arbitrary modes in arbitrary geometries in piezoelectric resonators." *IEEE Trans. Ultrason., Ferroelect., Freq. Contr., 59*(5), 1043-1060.

[2] S. S. Bedair, J. S. Pulskamp, R. G. Polcawich, R. Q. Rudy and J. Puder, "Thin-film piezoelectric transformers operating in harmonics of out-of-plane flexure modes," *2015 Transducers - 2015 18th International Conference on Solid-State Sensors, Actuators and Microsystems (TRANSDUCERS)*, Anchorage, AK, 2015, pp. 714-717.

[3] J. S. Pulskamp, R. Q. Rudy, S. S. Bedair, J. M. Puder, M. G. Breen and R. G. Polcawich, "Ferroelectric PZT MEMS HF/VHF resonators/filters," *2016 IEEE International Frequency Control Symposium (IFCS)*, New Orleans, LA, 2016, pp. 1-4.

[4] J. S. Pulskamp, S. S. Bedair, G. Ronald and S. A. Bhave, "Ferroelectric PZT RF MEMS resonators," *2011 Joint Conference of the IEEE International Frequency Control and the European Frequency and Time Forum (FCS) Proceedings*, San Fransisco, CA, 2011, pp. 1-6.

[5] Rudy, R.Q, et al.. "Piezoelectric Disk Flexure Resonator with 1 dB Loss." *2016 IEEE International Frequency Control Symposium*.

[6] T.B. Gabrielson. "Frequency Constants for Transverse Vibration Of Annular Disks". *The J. of the Acoust. Soc. of Amer.*, vol. 105, no. 6, pp. 3311-3317, June 1999.

[7] Puder, J.M., et al. (2017). "A General Analytical Formulation for the Motional Parameters of Acoustic Resonators." *Transactions on Ultrasonics, Ferroelectrics, and Frequency Control*, submitted.

[8] Puder, J. M., et.al., "Fundamental Limits of Disk Flexure Resonators," *2017 IEEE Intl. Fre. Cont. Symp*, accepted.

[9] Puder, J.M., et al. (2016). "Modeling of High-Electric Bias Field Induced Piezoelectric Nonlinearity." *2016 International Workshop on Acoustic Transduction Materials and Devices*.

[10] Yagnamurthy, S., et. al. (2011). "Mechanical and Ferroelectric Behavior of PZT-Based Thin Films." *J. Microelectromech. Syst., 20*(6), 1250-1258.

[11] Polcawich, Ronald G., and Jeffrey S. Pulskamp. "Additive processes for piezoelectric materials: Piezoelectric MEMS." MEMS materials and Processes Handbook (2011): 273-353.